Measurement of Heterogeneous Reaction Rates during Indium-Mediated Allylation

Isabel A. Olson, Anne M. Sessler, Jodi L. Connell, Esthefanie Giordano, Yessica Y. Baez Sosa, Salvador W. Zavaleta, and Walter J. Bowyer*

Department of Chemistry, Hobart and William Smith Colleges, Geneva, New York 14456

Received: December 16, 2008; Revised Manuscript Received: January 17, 2009

Indium-mediated allylation provides remarkable stereo- and regioselectivity, and it proceeds easily and in high yield in aqueous solutions. In spite of its widespread use, there have been few fundamental studies of this reaction. We have developed a photomicrographic technique for measuring rates of reaction of allyl halides at indium surfaces, and we describe the mathematical model for discriminating between diffusion and kinetic control. The measurements demonstrate that this reaction is diffusion controlled, and the minimum value of the heterogeneous rate constant is 1×10^{-3} cm s^{-1}. These results broaden the applicability of photomicroscopy for measuring heterogeneous rates of reactions that result in consumption of solid metals.

Introduction

Indium-mediated allylation (IMA) has proven to be a powerful and diverse tool for the formation of C−C bonds.[1−8] A general example is illustrated in Scheme 1. The reaction usually proceeds with high regio- and stereoselectivity, can often be performed in water, and proceeds under mild conditions. Few side reactions complicate the reactions, and overall yields are typically high. Variations in the electrophile and the organohalide have broadened the synthetic scope of IMAs, and they have been applied to the synthesis of a wide range of compounds including carbohydrates, natural products, and others.[9−16] The importance of the reaction to synthetic chemists is demonstrated by the regular appearance of reviews,[4−7] and innovative extensions continue to flourish; see, e.g., ref 9.

Thus, it is surprising that there have been few fundamental studies of these reactions. In this paper, we report the first measurements of the rate of the first step of IMA, the reaction of allyl bromide at indium surfaces. While electrochemical techniques offer a wide array of strategies for measuring electron transfer rates at electrode surfaces, there are relatively few techniques for measuring rates of other heterogeneous reactions, especially those at surfaces that are being consumed. Thus, the photomicrographic technique described represents an important addition to the relatively small repertoire of tools for measuring heterogeneous reaction rates.

In most synthetic applications, the indium-mediated reactions are performed under Barbier conditions, in which the indium, allyl bromide, and electrophile are reacted together in a single step. However, the reaction proceeds in two steps, as illustrated in Scheme 1.[2,16,17] The intermediacy of a discrete organoindium intermediate has been well demonstrated, but the structure of that intermediate is still debated. Scheme 1 illustrates the intermediate, **1**, preferred by Chan and his students.[18] Other possibilities include diallylindium(III) halide, allylindium(III) dihalide, allylindium sesquibromide, and triallylindium.[10,16−25]

IMAs are often regio- and stereoselective, and many authors have made clever use of that selectivity both to control the geometry of the products and to explore the mechanism of the reaction.[4,12,14−16,22−26] It is now firmly established that the indium intermediate coordinates with the electrophile and so determines the geometry of the final product. Because solvation can affect the geometry of the intermediate, a change of solvent (often from aqueous to organic) can reverse which regio- or stereoisomer is produced.[4,10,27]

Given the importance of IMA and the uncertainty of the structure of the organometallic intermediate, it is remarkable that there have been no studies of the rate of reaction of allyl bromide at indium surfaces. The kinetics of the overall reaction (i.e., both steps 1 and 2 in Scheme 1) have been studied qualitatively by measuring the time for completion of reactions (usually by monitoring with TLC); see, e.g., refs 14−16. Complementing these studies, competition reactions involving two different electrophiles in the same solution have been measured to test hypothetical mechanisms for the second step; see, e.g., ref 15. However, it is interesting that the kinetics of the second step have been studied while the first step, generally presumed to be rate determining,[14,16,26] has been ignored.

Three difficulties complicate the determination of rates of the formation of organometallic compounds at metal surfaces.[28−31] First, the initiation time is variable, so the time at which the reaction begins is not easily determined. Second, mass transport in a stirred heterogeneous system can be difficult to describe quantitatively. Third, even an apparently uniform surface may not react uniformly, so knowledge of the reactive surface area is difficult. The erosion of the surface that occurs during the reaction exacerbates this problem by continuously changing the surface area.[28−36]

The diversity and importance of reactions at surfaces make surface science a major discipline, and the power of *in situ* imaging of reactive surfaces for studies of the kinetics and mechanisms of reactions at surfaces has been demonstrated.[28,32−36] Along these lines, we described a novel method of quantifying the rate of formation of Grignard reagents using photomicrography.[28,31,32] A magnesium strip was placed in a cell that allowed microscopic *in situ* observation of the surface. Formation of Grignard reagent occurred at discrete sites, resulting in hemispherical pits in the magnesium. We derived the relationship between the rate of growth of pits (defined as the slope of a plot of pit radius vs time, dr/dt) and the rate of the reaction. This relationship, eq 1, allows calculation of the rate constants,

* Corresponding author.

10.1021/jp811111e CCC: $40.75
Published on Web 02/25/2009

SCHEME 1

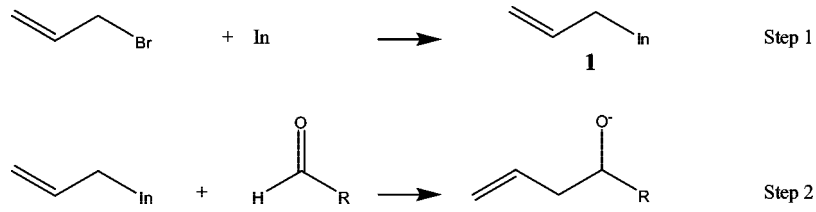

where k_s is the heterogeneous rate constant (cm s^{-1}), C^n is the concentration (mol cm^{-3}) of the organohalide raised to the order of reaction, n, and V_m is the volume of 1 mol of the metal.[28]

$$dr/dt = k_s C^n V_m \quad (1)$$

In contrast, if hemispherical diffusion to the reactive site controls the rate of formation of Grignard reagents, the plot of r vs t is not linear and the slope would be described by eq 2.

$$dr/dt = 8.9DC/r \quad (2)$$

D is the diffusion coefficient of the allyl halide in cm^2 s^{-1}.

Equation 1 accurately describes the Grignard reaction rates, allowing determination of rate constants as well as enthalpies and entropies of activation, and we proposed a surface-bound transition state.[28] Independent studies have recently supported our kinetic parameters[33] and our value for the enthalpy of activation.[37] Density functional theory (DFT) calculations supported a transition state only slightly different from the one we proposed.[37]

We now report similar studies on indium surfaces that further demonstrate the power of light microscopy in measuring rates of reactions at solid surfaces. We show that the reaction of allyl bromide at indium surfaces is diffusion controlled in 60% ethanol /40% water/0.1 M HCl.

Experimental Section

Image Recording and Analysis. A trinocular Nikon SMZ-U Zoom 1:10 microscope, Diagnostic Instruments monochromatic video camera, Spot version 4.6 software, and an MVI model NCL150 light source were used to obtain and make measurements on the photomicrographs. The calibration of the image system was confirmed each day by photographing a Meleemeter (Edmund Scientific) and measuring the line spacing.

Reagents. Indium powder (0.325 mesh, 99.99%) and indium foil (99.99%) were obtained from Alfa Aesar. Allyl halides were obtained from Acros Organics and passed down a short column of activated alumina before use. Deuterated solvents were obtained from Norell, Inc. All other reagents and solvents were obtained from Aldrich or Fisher Scientific and used as received. Reactions were performed at room temperature (22−24 °C) in 60% ethanol/40% water.

Measuring Reaction Rates. Photomicrography was used to quantify the rate of the reaction. In contrast to magnesium, indium metal is reactive toward allyl halides over the entire surface, and discrete pits are not observed. This may be because the In surface does not form an oxide layer to the same extent as Mg.[3] To simplify the geometry of the retreat, we constrained the reaction largely to a single surface of the indium (we quantify the success of the constraint below) by sandwiching the foil between two pieces of glass 2.5 × 3.5 cm cut from Corning Glassworks microscope slides. See Figure 1. A rectangle of indium foil (0.127 mm thick, approximately 2 × 4 mm) was sandwiched between the glass pieces so that a small amount of foil protruded from one side. The sandwich was wrapped tightly with Teflon tape (1/2 in. wide) to secure the indium foil in place without blocking the view of the indium foil through the glass. The protruding foil was carefully sliced off with a scalpel so that the remaining metal edge aligned precisely with the edge of the glass sandwich. The sandwich was then placed in the bottom of a home-built cylindrical Teflon cell (o.d. = 5 cm; i.d. = 4 cm; depth = 3 cm) with a lid machined to be tight fitting. See Figures 1−3. (After construction, each cell was cleaned, filled with acetone, and weighed to ±0.01 g. If no loss of acetone to evaporation was detected by remassing after 24 h, the cell was deemed to be sufficiently leakproof.)

The sandwich was placed in the cell, a small stir bar was placed on top of the sandwich, and 10 mL of the solvent/reagent mix was added to immerse the sandwich and stir bar. The image was quickly recorded, and the cell was capped.

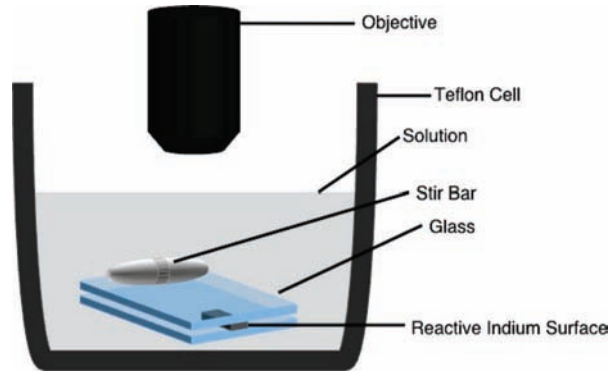

Figure 1. Diagram of the indium sandwich immersed in the allyl halide solution in a Teflon cell. For clarity, the Teflon tape binding the back portion of the sandwich is not illustrated.

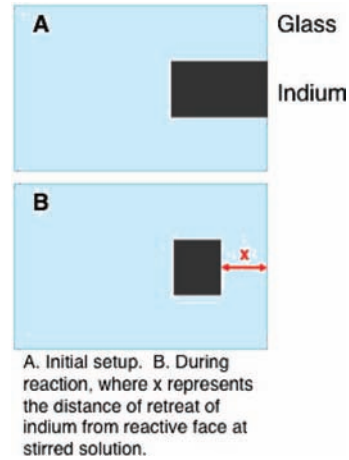

Figure 2. Indium sandwich viewed from above to illustrate the measurement of x, the distance of retreat of indium. The thickness of the static diffusion layer, δ, through which allyl bromide must diffuse from the well-stirred solution to the indium surface is equal to x.

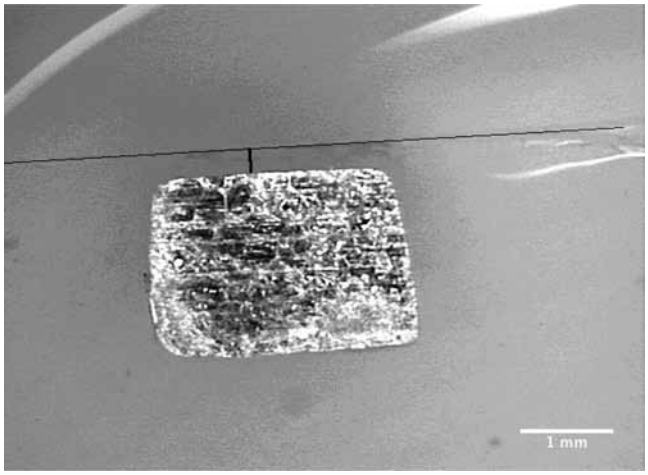

Figure 3. Photomicrograph of indium foil in glass sandwich during reaction with 0.10 M allyl bromide in 60% ethanol/40% water. The edge of the glass sandwich is enhanced by the lighter black line, while the heavier black line indicates the distance of retreat.

TABLE 1: Percent of Indium Recovered after Reaction: Calculated by Area in Photomicrograph or by Initial and Final Mass of Indium Strip[a]

[allyl Br]/M	% recovered by area	% recovered by mass	% lost from each face
0.17	38	35	5%
0.17	33	30	4%
0.1	62	48	16%
0.1	65	46	15%
0.01	89	88	1%
0.01	99	85	7%

[a] Calculated % of the indium thickness lost from each face contacting the glass. Determined for six pieces of indium foil at three different concentrations of allyl bromide.

Photomicrographs of the glass sandwich were taken at various intervals, ranging from 30 min to 24 h, by briefly removing the cover of the reaction cell, recording the image, replacing the solution with one freshly made, replacing the lid, and returning the cell to the stir plate for further reaction. Illumination only occurred for about 60 s during focusing and recording of each photograph and was not sufficient to change the temperature of the cell. The distance of the retreat from the edge was measured from the image at five locations across the reactive face with the Spot software. See Figure 2. Typically, the experiments were continued until the gap grew to 0.5−1 mm.

NMR Tube Reactions. In order to determine the stoichiometry of the reaction of indium with allyl halide, we performed the reaction in NMR tubes. Typically, 0.1−0.3 mmol of indium (mass determined to three significant figures) was weighed into a clean, dry NMR tube. The internal standard (methanol and/or tetramethylsilane) and deuterated solvent were then added, and a blank spectrum was recorded. A measured excess of allyl halide was added with a microsyringe, and the time = 0 spectrum was recorded. Additional spectra were run at intervals, and the tube was mixed in between spectra by rotating on a spindle to turn the tube end-over-end at 0.05 Hz.

NMR spectra were run on a 400 MHz Varian model 400MR NMR spectrometer using a relaxation delay of 10 s and a pulse angle of 15° in order to improve the accuracy of the integrations.

Electrochemical Measurements. A PARC 174 potentiostat and Kipp and Zonen $x-y$ recorder were used for the electrochemical measurements. The solvent was 60% ethanol/40% water/0.10 M HCl, and the electrode was a BioAnalytical Systems gold disk macroelectrode with a diameter of 1.63 mm. Background currents were demonstrated to be negligible by measurement in solutions with no analyte. Cyclic voltammograms were recorded to demonstrate diffusion control (constant $i_p\, v^{-1/2}$) as well as to select the correct range of voltages for the chronoamperometry. Diffusion coefficients were calculated from the chronoamperometric currents recorded over a range of 0.5−10 s. Solution concentrations were approximately 1 mM and prepared precisely to three significant figures.

Viscosity Measurements. We determined the viscosity of the solvent mixes in centistokes by measuring efflux time in triplicate with a calibrated Cannon-Frenske viscometer in a water bath at 24.8 °C. Values were converted to centipoise, cP, using the density of the solvent mix.

Theory. For allyl halide to react with indium, two processes must occur: (1) the halide must diffuse to the surface, and (2) bonds must be broken and formed as the reactants surmount the energy of activation barrier. If the energy of activation is sufficiently small, then diffusion will be rate limiting. If diffusion of halide from the solution to the surface controls the rate of reaction, the rate decreases as the thickness of the layer of static solution increases. Here, we derive the equations for the geometry of the indium/glass sandwich that describe the distance of retreat, x, of a reacting surface as a function of time under kinetic control and under diffusion control.

Kinetic Control. It is possible to describe the rate of reaction at the surface as a function of the volume of the indium metal that reacts:

$$dV/dt = \text{rate}(V_m) \tag{3}$$

V is the lost volume of indium (cm^3), t is the time of reaction (s), "rate" is the rate of reaction of indium with allyl halide at the surface (mol s^{-1}), and V_m is the volume of 1 mol of indium (15.7 cm^3 mol^{-1}).

At a single uniformly reactive surface, the volume of indium reacted is simply the product of the distance of retreat of the metal (x, measured perpendicular to the reacting surface), the width (y), and length (z) of the reacting surface, all measured in cm. A is the reactive surface area (yz) in cm^2.

$$V = xyz = xA \tag{4}$$

If the width and length of the reactive surface are constant, taking the derivative of both sides as a function of time yields

$$dV/dt = yz(dx/dt) = A(dx/dt) \tag{5}$$

For a heterogeneous reaction requiring significant activation energy, the rate law is

$$\text{rate} = k_s C^n A \tag{6}$$

where k_s is the heterogeneous rate constant (cm s^{-1} for a first order reaction), C is the bulk allyl halide concentration (mol cm^{-3}), and n is the order of reaction.

By substituting eq 5 into eq 3

$$A(dx/dt) = \text{rate}(V_m) \tag{7}$$

By substituting eq 6 into eq 7 and simplifying, the rate of retreat of the surface is

$$dx/dt = k_s C^n V_m \quad (8)$$

Thus, a plot x vs t would yield a straight line, and the heterogeneous rate constant can be determined from the slope. Not surprisingly, eq 8 is similar to eq 1.

Diffusion Control. On the other hand, if diffusion controls the rate, x vs t is not linear. Diffusion from a well-mixed solution through a quiescent layer of solution of thickness δ (cm) is described by[38]

$$\text{Flux} = ADC/\delta \quad (9)$$

"Flux" is the rate of arrival of allyl halide at the surface (mol s^{-1}).

Similar to eq 3 except including b, the stoichiometric ratio of moles of allyl halide reacting per mole of indium (mol allyl halide/mol indium) is

$$dV/dt = \text{Flux}(V_m)/b \quad (10)$$

Substituting eqs 5 and 9 into eq 10

$$A(dx/dt) = \text{Flux}(V_m)/b = (ADC/\delta)(V_m)/b \quad (11)$$

Simplifying eq 11 yields

$$dx/dt = DCV_m/b\delta \quad (12)$$

Because of the geometry of the indium/glass sandwich, the distance of metal retreat is equal to the quiescent solution layer thickness (see Figure 2)

$$x = \delta \quad (13)$$

Substituting eq 13 into eq 12

$$dx/dt = DCV_m/bx \quad (14)$$

With the initial condition that $x = 0$ when $t = 0$, integrating eq 14 yields

$$x = (2DCV_m/b)^{1/2} t^{1/2} \quad (15)$$

In contrast to kinetic control, plotting x vs $t^{1/2}$ yields a straight line with slope m

$$m = (2DCV_m/b)^{1/2} = (2DV_m b)^{1/2} C^{1/2} \quad (16)$$

Taking the log of each side and rearranging

$$\log(m) = \log(2DV_m/b)^{1/2} + 1/2 \log(C) \quad (17)$$

Results

Selection of Solvent. One important advantage of IMA is that the reaction can be performed in aqueous solutions. Although reactants are not usually soluble, many synthetic chemists use water as their solvent. However, it is not possible to do kinetic studies without knowing and controlling the concentrations of reactants. We chose 60% ethanol/40% water, a mix that allows us to control the allyl bromide concentration up to 0.2 M at room temperature. Furthermore, organic/aqueous solvent mixtures are used by many synthetic chemists.[14−16,39,40]

Figure 3 is a photomicrograph of a piece of indium foil reacting with 0.10 M allyl bromide in 60% ethanol/40% water after 48 h. The edge of the glass sandwich, enhanced in this photomicrograph by the lighter black line, can be seen approximately 0.3 mm above the top edge of the indium. At time = 0, the edge of the indium and the glass were aligned, so the distance of retreat over 48 h, x, is the distance from the glass edge to the indium edge. A single measurement (out of five replicates) of x is illustrated here by the heavier black line.

Characterization of Products. To confirm that we are indeed studying the reaction of interest, we have isolated and identified by NMR the homoallylic alcohol expected from the reaction of allyl bromide, indium, and benzaldehyde. We have also confirmed that the solvent and other reagents (aqueous ethanol, HCl, and aldehydes) do not react with indium surfaces in the absence of allyl bromide, even after prolonged contact.

Success of Constraining Reactivity to a Single Face. The equations derived above require that the retreat, x, is measured on a face that is perpendicular to the dimension x. We have confirmed this requirement in several ways.

The ethanol/water mix enters into the glass sandwich by capillary action, immersing all four edges in allyl halide solution. Thus, all four edges do react with allyl halide. Qualitatively, this is apparent by the rounded corners of the indium foil in Figure 3, which were cut at close to 90° before the reaction was begun. To quantify this effect, we measured rates of retreat on all four edges; slopes on the back and side edges averaged from 0 to 40% those of the edge closest to the end of the sandwich. This is not surprising if diffusion controls the reaction rate (discussed further below) since allyl halide must diffuse further to reach the back and side edges compared to the top edge.

Further supporting the applicability of the model's geometry, the top edge of the indium remains normal to the dimension of retreat, x, over most of its length. When measuring x, we choose five locations along the straight portion of the indium edge.

Determining reactivity on the faces in contact with the glass slides is more challenging since retreat there would not be apparent in the photomicrograph. Thus, after reacting the indium/glass sandwiches in solutions of varying concentrations of allyl bromide for varying times, we measured the surface area of the remaining foil from the micrograph. From this we calculate the percent area lost, which represents the amount lost to reactions along all the edges of the foil. We also disassemble the sandwich, clean and dry the indium, and determine its mass. By comparing its final mass to its initial mass, we calculate the total amount of indium lost. From these values, it is possible to calculate the percent of the thickness of the foil that was lost from each face. After doing this with six pieces of indium foil, we find that on average only 4% of the thickness of the foil, or 5 μm, is lost from each of the two faces that contacts the glass.

Finally, to qualitatively confirm the result in Table 1 that relatively little of the indium is lost from the faces contacting the glass slides, we imbedded the pieces of reacted indium foil

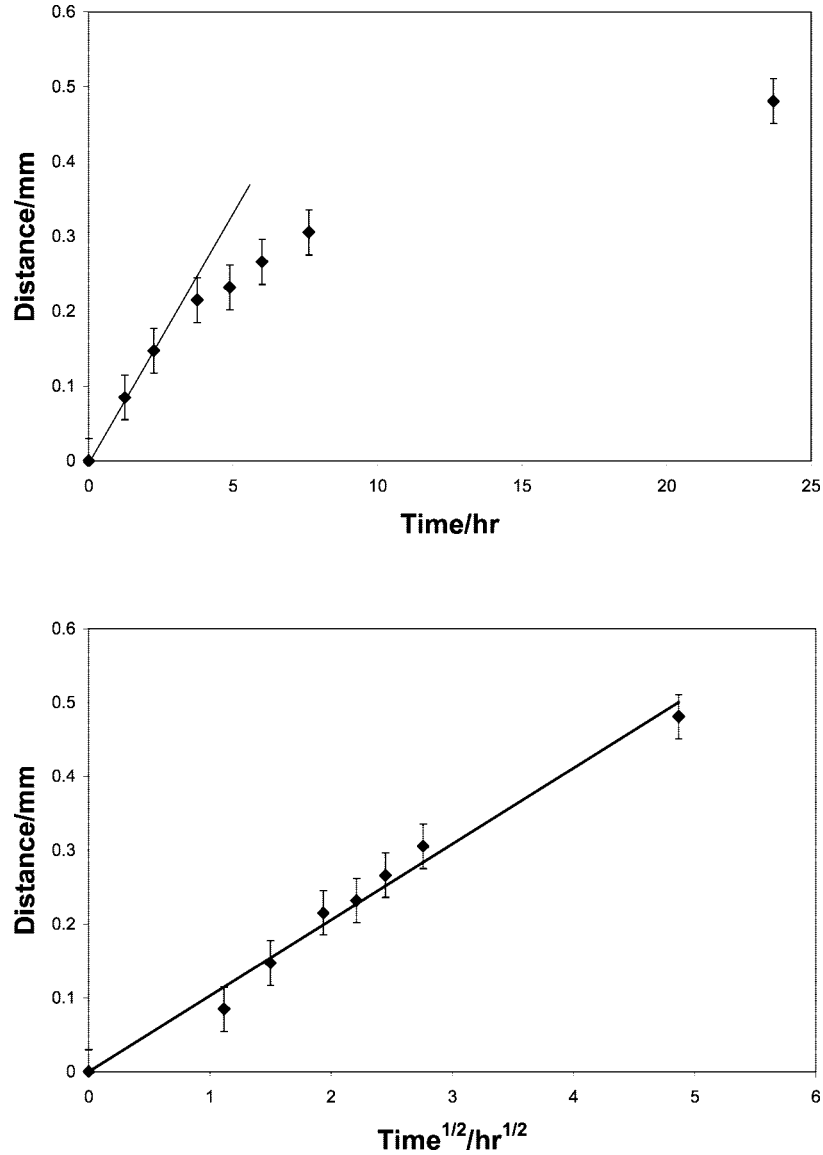

Figure 4. Plot of x vs t (upper) and x vs $t^{1/2}$ (lower) for an indium surface reacting in 0.20 M allyl bromide/0.10 M HCl/60% ethanol/40% water. Error bars represent ±one standard deviation based on five replicates at each time.

in epoxy and sliced them in order to observe a cross section of the reactive surface. In all cases, although the corners were rounded, most of the surface remained normal to dimension x. Thus, we conclude that measuring the rate of retreat of the edge as viewed through the microscope does indeed represent the rate of retreat of the face.

Diffusion vs Kinetic Control. Equation 8 predicts that if the reaction of allyl bromide at indium surfaces is kinetically controlled, the plot of retreat of the surface, x, vs time will be linear. In contrast, eq 15 predicts that if the reaction is diffusion controlled, a plot of x vs the square root of time, $t^{1/2}$, will be linear. After many replicates, the retreat of the indium surface consistently exhibits a concave downward curve when x is plotted vs t. Qualitatively, this is consistent with diffusion control because as the gap becomes larger, the diffusion layer becomes thicker and flux decreases. More quantitatively, the same data yield a straight line when x is plotted vs $t^{1/2}$. For example, Figure 4 illustrates the retreat of an indium surface reacting in 0.20 M allyl bromide. The upper graph is x plotted vs time, while the lower graph is the same data plotted vs the square root of time. Each point represents five replicates along the retreating indium edge. While the first few points in the upper graph appear reasonably linear, the curvature becomes apparent after 4 h. In contrast, the linearity of the lower graph continues to the end of the experiment at 24 h.

In further support of diffusion control, if the kinetic model is assumed and a straight line is forced through the early points of the x vs t plots, there are two problems with the resulting data. First, there is much less reproducibility in the slopes compared to those using x vs $t^{1/2}$. Second, the resulting slopes suggest that the order of the reaction is 0.3 with respect to allyl bromide, an unlikely value.

Thus, only the diffusion control model is consistent with our results, and further data analysis is done using this model. Equation 16 predicts that the slope of the plot of x vs $t^{1/2}$ is $(2DCV_m/b)^{1/2}$. We have calculated slopes of x vs $t^{1/2}$ for 35 experiments at concentrations of allyl bromide ranging from 0.005 to 0.2 M and used the slopes of these lines to calculate D/b. Consistent with the hypothesis of diffusion control, the values of D/b are independent of allyl bromide concentration, and the average value is 5.3×10^{-6}. The confidence range is $\pm 0.8 \times 10^{-6}$ at the 95% confidence. (For the experimental determination of b and calculation of D, *vide infra*.)

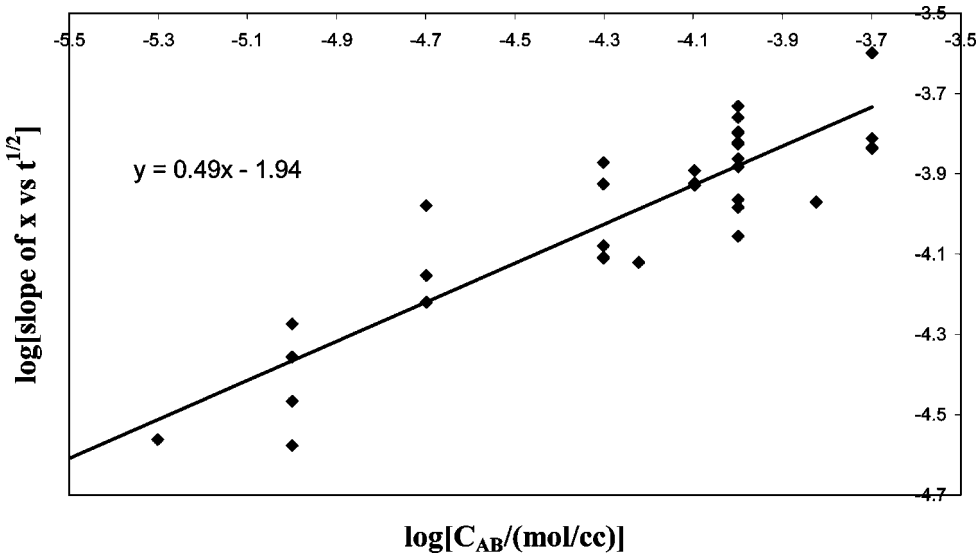

Figure 5. Log−log plot for 35 experiments with allyl bromide ranging from 0.0050 to 0.20 M. [HCl] = 0.10 M in all cases.

TABLE 2: Stoichiometric Ratio of Moles of Allyl Halide Reacting with In

mmol In	mmol allyl bromide	mmol allyl iodide	% allyl halide reacted	allyl halide:In
0.124	0.252	0	75.9	1.54
0.169	0.252	0	94.6	1.41
0.247	0.252	0.249	76.0	1.53

Equation 17 predicts that if the log of the slopes is plotted vs the log of the allyl bromide concentration, a straight line with a slope of 0.5 will result. Figure 5 illustrates this plot with a best fit line of $m = 0.49$, again confirming diffusion control for this reaction under these conditions. Further, the intercept of the line in Figure 5 allows calculation of D/b, whose value is consistent with the average calculated above using eq 16.

To determine the value of D for allyl bromide using eq 16, the value of b, the stoichiometric ratio of allyl bromide to indium, must be known. This conversion is necessary because the loss of indium is experimentally measured by photomicrography. To convert the rate of disappearance of indium into the flux of allyl halide, the stoichiometry of the reaction is needed (eq 10). We determine the stoichiometry with a series of reactions performed in an NMR tube.

NMR Tube Experiments To Determine *b*. Araki[2,10,41] has determined the stoichiometry of indium-mediated allylation, but only in the presence of benzaldehye or other electrophiles (Scheme 1, steps 1 and 2). Chan[18,19] has described the reaction of allyl bromide and indium in D_2O in NMR tubes to study the intermediate, but he has not reported the stoichiometry.

We have done a series of reactions in NMR tubes, using integration and inert internal standards to monitor the quantity of allyl bromide and/or allyl iodide reacting with indium. Indium is reacted with excess allyl halide in 1.66 mL of deuterated 60% ethanol/40% water. The doublet at 1.7 ppm characteristic of a single indium intermediate[18] rapidly appears, and its area increases at the expense of the peaks of allyl halide. We measure the amount of allyl halide consumed as a function of time until all of the indium has reacted and the area of the remaining allyl halide is constant with time. When the tubes are efficiently mixed at room temperature, time for completion of the reaction ranges from 10 to 30 min. In Table 2, we report the ratio of allyl halide consumed to indium upon completion of the reaction. From these experiments, two indium atoms consume three allyl halide molecules.

Because the time scale of the experiment can affect the apparent stoichiometry of a reaction if several steps are involved, it is important to note that the time scale for the NMR measurement of b is comparable to the time scale of the experiments in the sandwiches when the gap is close to its maximum, 0.5−1 mm. As reactants, intermediates, and products diffuse through the gap, the time scale of the experiment is estimated from the approximation[38] that the diffusion layer thickness, x, corresponds to $(Dt)^{1/2}$. With a typical value of D (5×10^{-6} cm^2 s^{-1}) and a gap of 0.8 mm, the time scale of the experiment is about 20 min. Of course, early in the experiment when the gaps are smaller, the time scale is much shorter. The linear plots of x vs $t^{1/2}$ (Figure 4) are consistent with a stoichiometry that does not change over the range of time scales represented in the sandwich experiments. Thus, the stoichiometry measured by the NMR experiments is the same as that occurring in the indium/glass sandwiches.

Effect of Acid and Electrophile on Rate. We explored the effect of the concentration of HCl and benzaldehyde on the rate of the reaction of indium.

It has been reported that hydrochloric acid accelerates or catalyzes IMA; see, e.g., ref 16. To explore this effect, we varied the concentration of HCl from 0 to 0.1 M at a variety of allyl bromide and benzaldehyde concentrations in 46 different experiments. For concentrations of HCl from 0.015 to 0.1 M, we found no effect of [HCl] on the rate of retreat. At concentrations lower than 0.015 M, rates of reaction decreased and became less reproducibile. For example, at 0 M HCl, the average reaction rate was 20−30% of that when the HCl concentration was greater than 0.015 M. The viscosity of the solvent is almost unaffected by the HCl (at 24.8 °C, $\eta = 2.49$ cP with 0.1 M HCl compared to 2.45 cP without HCl), so diffusion rates should also be unaffected. We suspect that in the absence of acid, indium hydroxide precipitates on the indium surface, hindering the reaction. All values of D reported in this paper were obtained in 0.10 M HCl.

Similarly, we measured reaction rates at 0−0.20 M benzaldehyde and found no effect on reaction rate. Use of other electrophiles, for example, benzophenone and cinnamaldehyde, also had no effect on reaction rates.

Reaction Rate of Allyl Iodide Compared to Allyl Bromide. Typically, organoiodides are more reactive toward metals than are organobromides, and it has been noted that this is true of

IMA; see, e.g., ref 10. The difference of reactivity may result from the increased driving force (since C−Br bonds are stronger than C−I bonds), more rapid initiation, or lower energy of activation.[28]

We performed a series of experiments measuring the rate of reaction of indium with a range of allyl iodide concentrations from 0.01 to 0.2 M. Rates of reaction of allyl iodide are not significantly different from those of allyl bromide. Again, plots of x vs t were curved downward, while plots of x vs $t^{1/2}$ were linear. Also, a plot of the log of slopes vs log of allyl iodide concentration yielded a slope of 0.44, close to 0.5. These data are consistent with diffusion control of the rate of reaction of allyl iodide and allow calculation of the D of allyl iodide.

Values of *D*. Based upon all of these experiments, we conclude that the reaction of allyl bromide and allyl iodide at indium surfaces is diffusion controlled. Using the value of $b = 1.5$, we calculate an average value of D for allyl bromide in 60% ethanol/40% water/0.10 M HCl at 22−24 °C to be 7.9 ($\pm$1) $\times$ 10^{-6} cm^2 s^{-1}. A similar calculation for allyl iodide yields a D of 8.7 $\times$ 10^{-6} cm^2 s^{-1}.

We were unable to find reported values for the value of D of allyl halides in our solvent mix, but the D of allyl bromide in DMF has been reported to be 13.5 $\times$ 10^{-6} cm^2/s.[42] We determined the viscosity of 60% ethanol/40% water/0.1 M HCl to be 2.49 ($\pm$0.02) cP at 24.8 °C. Using the Stokes−Einstein equation to adjust for the viscosity of our solvent mix compared to that of DMF (0.796 cP),[43] the expected value of D for allyl halide in ethanol/water would be 4.3 $\times$ 10^{-6} cm^2 s^{-1}, lower but still in reasonable agreement with our value.

Also, we found reported values of D for seven slightly polar molecules similar in size to allyl bromide (benzaldehyde, chlorobenzene, 1,2,4-trichlorobenzene, nitrobenzene, bromobenzene, benzoquinone, and *N*,*N*,*N*′,*N*′-tetramethyl-*p*-phenylene diamine) in 100% ethanol.[44−47] We again adjusted those values for viscosity (using the viscosity of ethanol, $\eta = 1.08$ cP)[43] and found an average value of 8.2 $\times$ 10^{-6} cm^2 s^{-1}, in very good agreement with our value for allyl bromide.

Finally, we used chronoamperometry to determine the D in our solvent mix for benzoquinone, which is similar in size and polarity to allyl bromide (and which undergoes a well-behaved two-electron reduction in aqueous solutions). By chronoamperometry, the limiting current was proportional to the square root of time over the time range measured (0.5−10 s). We determined the value of D to be 13 $\times$ 10^{-6} cm^2/s, slightly larger than our value for the D of allyl bromide.

Minimum Value of k_s. As illustrated in the upper graph in Figure 4, the plot of x vs t begins with a relatively high slope, and the first few points often appear linear. At very short times, it is conceivable that the distance of retreat is so small that the diffusion is faster than the kinetic limit of the reaction. If so, one could measure the retreat very early in the process to determine k_s. Unfortunately, the limits of resolution of the microscope and the precision in aligning the indium foil in the glass sandwich preclude a rigorous test. Nevertheless, it is possible to take the highest slopes measured early in our experiments and calculate an apparent value of k_s using eq 8. This apparent k_s represents the minimum possible value for the actual k_s.

If we assume the reaction is first order in allyl bromide under kinetic control, it is possible to calculate the minimum value of k_s to be 1 $\times$ 10^{-3} cm s^{-1}. Interestingly, this value is 10 times larger than the largest k_s for the reaction of organobromides at magnesium surfaces in tetrahydrofuran to form Grignard reagents.[28]

Conclusion

We have developed a photomicrographic technique for measuring rates of reaction of allyl halides at indium surfaces. Measurements using this technique lead to the conclusion that the reactions of allyl bromide and allyl iodide at indium surfaces are diffusion controlled under our conditions, and the diffusion coefficients are 7.9 ($\pm$1) $\times$ 10^{-6} cm^2 s^{-1} for allyl bromide and 8.7 $\times$ 10^{-6} cm^2 s^{-1} for allyl iodide. The minimum value of the heterogeneous rate constant, k_s, is 1 $\times$ 10^{-3} cm s^{-1}. Perhaps most importantly, these results broaden the applicability[28,35] of photomicroscopy for measuring heterogeneous rates of reactions that result in consumption of solid metals. While electrochemical techniques offer a wide array of strategies for measuring electron transfer rates at electrode surfaces, there are relatively few techniques for measuring rates of other heterogeneous reactions.

Acknowledgment. This material is based upon work supported by the National Science Foundation under Grant No. CHE-0653311. We thank Richard Bolton and Kathy Slentz of Hobart and William Smith Colleges for technical assistance.

References and Notes

(1) Chao, L. C.; Rieke, R. D. *J. Org. Chem.* **1975**, *40*, 2253–2255.
(2) Araki, S.; Ito, H.; Butsugan, Y. *J. Org. Chem.* **1988**, *53*, 1831–1833.
(3) Li, C. J.; Chan, T. H. *Tetrahedron Lett.* **1991**, *32*, 7017–7020.
(4) (a) Paquette, L. A. In *Green Chemistry: Frontiers in Benign Chemical Synthesis and Processing*; Antas, P., Williamson, T., Eds.: Oxford University Press: Oxford, 1998. (b) Paquette, L. A. *Synthesis* **2003**, *5*, 765–774.
(5) Podlech, J.; Maier, T. C. *Synthesis* **2003**, *5*, 633–655.
(6) Nair, V.; Ros, S.; Jayan, C. N.; Pillai, B. S. *Tetrahedron* **2004**, *60*, 1959–1982.
(7) Li, C. J. *Chem. Rev.* **2005**, *105*, 3095–3165.
(8) Augé, J.; Lubin-Germain, N.; Uziel, J. *Synthesis* **2007**, *12*, 1739–1764.
(9) (a) Schneider, U.; Ueno, M.; Kobayashi, S. *J. Am. Chem. Soc.* **2008**, *130*, 13824–13825. (b) Fujimoto, T.; Endo, K.; Tsuji, H.; Nakamura, M.; Nakamura, E. *J. Am. Chem. Soc.* **2008**, *130*, 4492–4496.
(10) Araki, S.; Shimizu, T.; Johar, P. S.; Jin, S. J.; Butsugan, Y. *J. Org. Chem.* **1991**, *56*, 2538–2542.
(11) Araki, S.; Hirashita, T.; Shimizu, H.; Yamamura, H.; Kawai, M.; Butsugan, Y. *Tetrahedron Lett.* **1996**, *37*, 8417–8420.
(12) Chan, T. H.; Isaac, M. B. *Pure Appl. Chem.* **1996**, *68*, 919–924.
(13) Keh, C. C. K.; Wei, C.; Li, C. J. *J. Am. Chem. Soc.* **2002**, *125*, 4062–4063.
(14) Paquette, L. A.; Bennett, G. D.; Isaac, M. B.; Chhatriwalla, A. *J. Org. Chem.* **1998**, *63*, 1836–1845.
(15) Paquette, L. A.; Rothhaar, R. R. *J. Org. Chem.* **1999**, *64*, 217–224.
(16) Kim, E.; Gordon, D. M.; Schmid, W.; Whitesides, G. M. *J. Org. Chem.* **1993**, *58*, 5500–5507.
(17) Araki, S.; Ito, H.; Katsumura, N.; Butsugan, Y. *J. Organomet. Chem.* **1989**, *369*, 291–296.
(18) (a) Chan, T. H.; Yang, Y. *J. Am. Chem. Soc.* **1999**, *121*, 3228–3229. (b) Yang, Y.; Chan, T. H. *J. Am. Chem. Soc.* **2000**, *122*, 402–403.
(19) (a) Law, M. C.; Cheung, T. W.; Wong, K.-Y.; Chan, T. H. *J. Org. Chem.* **2007**, *72*, 923–929. (b) Miao, W.; Chung, L. W.; Wu, Y. D.; Chan, T. H. *J. Am. Chem. Soc.* **2004**, *126*, 13326–13334.
(20) Xu, B.; Mashuta, M. S.; Hammond, G. B. *Angew. Chem., Int. Ed. Engl.* **2006**, *45*, 7265–7267.
(21) Miao, W.; Lu, W.; Chan, T. H. *J. Am. Chem. Soc.* **2003**, *125*, 2412–2413.
(22) Lu, W.; Chan, T. H. *J. Org. Chem.* **2001**, *66*, 3467–3473.
(23) Chung, W. J.; Higashiya, S.; Oba, Y.; Welch, J. T. *Tetrahedron* **2003**, *59*, 10031–10036.
(24) Isaac, M. B.; Chan, T. H. *Tetradedron Lett.* **1995**, *36*, 8957–8960.
(25) Hirashita, T.; Daikoku, Y.; Osaki, H.; Ogura, M.; Araki, S. *Tetrahedron Lett.* **2008**, *49*, 5411–5413.
(26) Li, J.; Zha, Z.; Sun, L.; Zhang, Y.; Wang, Z. *Chem. Lett.* **2006**, *35*, 498–499.
(27) Araki, S.; Shiraki, F.; Tanaka, T.; Nakano, H.; Subburaj, K.; Hirashita, T.; Yamamura, H.; Kawai, M. *Chem. Eur. J.* **2001**, *7*, 2784–2790.

(28) Beals, B. J.; Bello, Z. I.; Cuddihy, K. P.; Healy, E. M.; Koon-Church, S. E.; Owens, J. M.; Teerlinck, C. E.; Bowyer, W. J. *J. Phys. Chem. A* **2002**, *106*, 498–503.
(29) Rogers, H. R.; Hill, C. L.; Fujiwara, Y.; Rogers, R. J.; Mitchell, H. L.; Whitesides, G. M. *J. Am. Chem. Soc.* **1980**, *102*, 217–226.
(30) Rogers, H. R.; Deutch, J.; Whitesides, G. M. *J. Am. Chem. Soc.* **1980**, *102*, 226–231.
(31) Teerlinck, C. E.; Bowyer, W. J. *J. Org. Chem.* **1996**, *61*, 1059–1064.
(32) Koon, S. E.; Oyler, C. E.; Hill, J. H. M.; Bowyer, W. J. *J. Org. Chem.* **1993**, *58*, 3225.
(33) Simuste, H.; Panov, D.; Tuulmets, A.; Nguyen, B. T. *J. Organomet. Chem.* **2005**, *690*, 3061–3066.
(34) Wittstock, G.; Burchardt, M.; Pust, S. E.; Shen, Y.; Zhao, C. *Angew. Chem., Int. Ed. Engl.* **2007**, *46*, 1584–1617.
(35) Jones, C. E.; Macpherson, J. V.; Unwin, P. R. *J. Phys. Chem. B* **2000**, *104*, 2351–2359.
(36) Greenwell, H. C.; Bindley, L. A.; Unwin, P. R.; Holliman, P. J.; Jones, W.; Coveney, P. V.; Barnes, S. L. *J. Cryst. Growth* **2006**, *294*, 53–59.
(37) Jasien, P. G.; Abbondondola, J. A. *J. Mol. Struct. (Theochem)* **2004**, *671*, 111–118.
(38) Bard, A. J.; Faulkner, L. R. *Electrochemical Methods*; Wiley: New York, 1980; p 119−136.
(39) Vilaivan, T.; Winotapan, C.; Banphavichit, V.; Shinada, T.; Ohfune, Y. *J. Org. Chem.* **2005**, *70*, 3464–3471.
(40) Yi, X. H.; Meng, Y.; Hua, X. G.; Li, C. J. *J. Org. Chem.* **1998**, *63*, 7472–7480.
(41) Hirashita, T.; Kamei, T.; Horie, T.; Yamamura, H.; Kawai, M.; Araki, S. *J. Org. Chem.* **1999**, *64*, 172–177.
(42) Occhialini, D.; Pedersen, S. U.; Daasbjerg, K. *J. Electroanal. Chem.* **1994**, *369*, 39–52.
(43) Mann, C. K. In *Electroanalytical Chemistry, a Series of Advances*; Bard, A. J., Ed.; Dekker: New York, 1969; Vol. 3, pp 57−134.
(44) Terazima, M.; Okamoto, K.; Hirota, N. *J. Chem. Phys.* **1995**, *102*, 2506–2515.
(45) Chan, T. C.; Chen, N.; Lu, J. G. *J. Phys. Chem. A* **1998**, *102*, 9087–9090.
(46) Fiedel, H. W.; Schweiger, G.; Lucas, K. *J. Chem. Eng. Data* **1991**, *36*, 169–170.
(47) Klymenko, O. V.; Evans, R. G.; Hardacre, C.; Svir, I. B.; Compton, R. G. *J. Electroanal. Chem.* **2004**, *571*, 211–221.

JP811111E